

# Pulsatile blood flow in total cavopulmonary connection: a comparison between Y-shaped and T-shaped geometry

Hamidreza Rajabzadeh-Oghaz<sup>1</sup> · Bahar Firoozabadi<sup>1</sup> · Mohammad Said Saidi<sup>1</sup> · Mojdeh Monjezi<sup>1</sup> · Mohammad Ali Navabi Shirazi<sup>2</sup> · Elaheh Malakan Rad<sup>3</sup>

Received: 28 March 2014 / Accepted: 26 March 2016 / Published online: 23 April 2016  
© International Federation for Medical and Biological Engineering 2016

**Abstract** Single-ventricle anomaly is a hereditary heart disease that is characterized by anatomical malformations. The main consequence of this malformation is desaturated blood flow, which without proper treatment increases the risk of death. The classical treatment is based on a three-stage palliative procedure which should begin from the first few days of patient's life. The final stage is known as Fontan procedure, in which inferior vena cava is directly connected to pulmonary arteries without going through the ventricle. This connection is called total cavopulmonary connection (TCPC). After surgery, the single ventricle supplies adequate and saturated systemic blood flow to the body; however, TCPC contains low pressure and low flow pulsatility. To overcome this problem, a new method is proposed wherein pulsatile blood will be directed to the TCPC through the stenosed main pulmonary artery. In this study, through the use of Computational Fluid Dynamics, T-shaped (MRI-based) and Y-shaped (computer-generated) geometries are compared in order to determine the influence of this modification on pulsation of blood flow as well as energy loss in pulmonary arteries. The results indicate that energy loss in Y-shaped geometry is far less than T-shaped geometry, while the difference in flow pulsatility is insignificant.

**Keywords** Single ventricle · Fontan surgery · Total cavopulmonary connection (TCPC) · Fluid structure interaction (FSI)

## Abbreviation

TCPC	Total cavopulmonary connection
RPA	Right pulmonary artery
LPA	Left pulmonary artery
IVC	Inferior vena cava
SVC	Superior vena cava
PA	Pulmonary artery
PI	Pulsatility index
PF	Pulsatile flow
MRI	Magnetic resonance imaging
FSI	Fluid structure interaction

## 1 Introduction

Based on the report of National Birth Defect Prevention Network in USA, 2.3 per 10,000 babies born with anatomical malformations such as heart valves atresia, stenosis, under development right ventricle or hypoplastic left ventricle [16]. These children mainly born cyanosed because their oxygenated (red) and deoxygenated (blue) blood are mixed together. Desaturated and sometimes inadequate systemic blood flow is the main consequence of this malformation which without any treatment increases the risk of mortality. Some single-ventricle defects can be treated using three-stage palliative operations from the first few days to the next few years of patient's life. The first stage of the surgery is called Norwood Procedure, which is performed just a few days after the child's birth. The objective of the first stage is providing unobstructed blood flow from single ventricle to the systemic circulation. In this stage,

✉ Bahar Firoozabadi  
Firoozabadi@sharif.edu

<sup>1</sup> Department of Mechanical Engineering, Sharif University of Technology, Tehran, Iran

<sup>2</sup> Department of Pediatric Cardiac Surgery, Children's Medical Center, Tehran University of Medical Sciences, Tehran, Iran

<sup>3</sup> Department of Pediatric Cardiology, Children's Medical Center, Tehran University of Medical Sciences, Tehran, Iran

the blood flow for pulmonary arteries (PA) is supplied by placing a modified Blalock-Taussig shunt between repaired aorta and pulmonary arteries. After 6 months, when the patient becomes progressively more cyanotic, bidirectional Glenn operation is performed. This operation also reduces the single ventricle's workload by directly connecting the superior vena cava (SVC) to the pulmonary artery. In other words, using this connection half of the deoxygenated blood is directed to the lungs without passing through the single ventricle. The final operation is performed when the patient's lungs are matured. In this operation, inferior vena cava (IVC) is disconnected from the heart and instead redirected to the pulmonary arteries. This setup practically directs blood flow from SVC and IVC to directly enter pulmonary arteries without passing through the heart [5].

Most institutions have claimed that 95 % of patients after surgical intervention would probably have their normal life; however, they are susceptible to numerous long-term complications [2].

Numerical and clinical studies have demonstrated that the structure of TCPC has crucial role in energy loss and consequently in health of patients after surgery. Researchers have proved that high energy loss in TCPC has harmful effects on respiratory system. In addition, abnormal shear stress on the vessels contributes in thrombus formation, which cannot be neglected [2]. Some clinical studies such as Krishnakutty et al. [10], Fogel et al. [4] and Hjortdal et al. [8] investigated the difference of hemodynamics of blood flow in different TCPC anatomies.

In recent decades, the developments in computational fluid dynamics (CFD) tools have been provided beneficial means to simulate cardiovascular systems. Numerical researches [3, 11–13] have demonstrated that geometrical characteristics of TCPC are greatly effective in determining the efficacy of the operation. For instance, not only does an anatomy with high pressure drop causes lower oxygen saturation, especially under exercise condition, but also can lead to higher risk of thrombus formation and eventually postoperative mortality. Because of this significant importance of geometry optimization, Pekkan et al. [17] have introduced a new tool which can optimize the geometry more efficiently, compared to existing traditional CAD systems. They have shown that utilization of free-form haptic anatomy editing tool (SURGEM) eliminates the time-consuming phase of making a desired geometry using computer-aided design systems. Thus, patient-specific simulation before the surgical procedure can be extremely valuable in choosing an optimized TCPC geometry.

Investigation on T-shaped geometry demonstrated that the collision of IVC and SVC flows is the most important reason for high energy loss occurring in the TCPC. Marsden et al. [13, 23] proposed that pressure drop and energy loss decreases significantly by utilization of a Y-shaped

graft. In this procedure, IVC flow is directed to pulmonary arteries by placing a Y-shaped graft.

Another postoperative complication that these patients are facing is non-pulsatile blood flow in pulmonary arteries, which no practical solution has been found yet. Throckmorton et al. [20] utilized a pump to facilitate the blood flow in circulatory system; however, it is not an interesting solution due to the utilization of an external device in the body. Recently, several studies are advocated to the potential benefits of leaving pulsatile sources of antegrade pulmonary blood flow after bidirectional cavopulmonary anastomosis (BCPA) procedure [1, 7, 24]. Wal et al. [21] represented that by adding accessory pulsatile flow, the mean pulmonary artery pressure and oxygen saturation increase significantly and no pulmonary hypertension develops. They showed that long-term survival following Fontan with accessory pulsatile flow is significantly higher than the conventional Fontan and associates with better pulmonary artery growth. The idea of directing a pulsatile flow through stenosed PA with specific anatomy has been numerically tested by Ghoreyshi et al. [6] and Rajabzadeh et al. [18]. They demonstrated that this new idea increases the pulsatility of the pulmonary blood flow significantly; however, it increases the energy loss in TCPC. In order to reduce the energy loss that imposed by adding the pulsatile flow, Rajabzadeh Oghaz et al. [14] proposed a novel idea in which an elastic membrane is placed at the main pulmonary artery. This membrane fluctuates because of high gradient pressure that is imposed from univentricular heart. They proposed that the membrane can be constructed by sewing the leaflets of repaired pulmonary valve (three cups) together.

In current study, the new idea of adding pulsatile flow is taken to test using both T-shaped and Y-shaped geometry. Because of importance of vessel-wall compliance on the numerical results [15], this study is conducted using FSI (Fluid Structure Interaction) approach. Similar to previous researches [6], flow pulsatility along with energy loss are determined through the simulations.

## 2 Materials and Methods

### 2.1 Geometric morphology and material

The geometry of T-shaped model is constructed by MRI images, taken from a 9-year-old girl's thorax after a successful extra-cardiac Fontan surgery. It should be mentioned that approval of institutional committee of ethics on research is obtained. T-shaped configuration of TCPC is obtained by image processing of sequential MRI images with 6 mm thickness, shown in Fig. 1. In this figure, the process of image segmentation and geometry

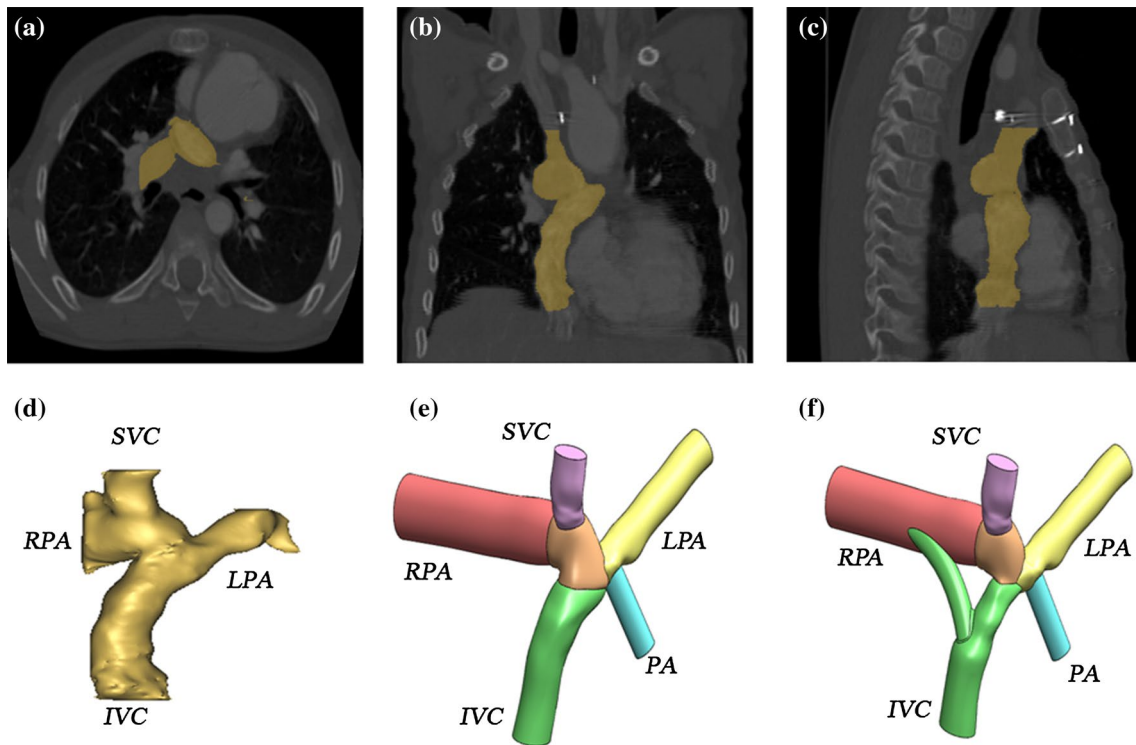


**Fig. 1** Sequence process of construction of T-shaped and Y-shaped geometries, **a** coronal plane, **b** axial plane, **c** sagittal plane, **d** 3D reconstruction part, **e** T-shaped geometry, **f** Y-shaped geometry

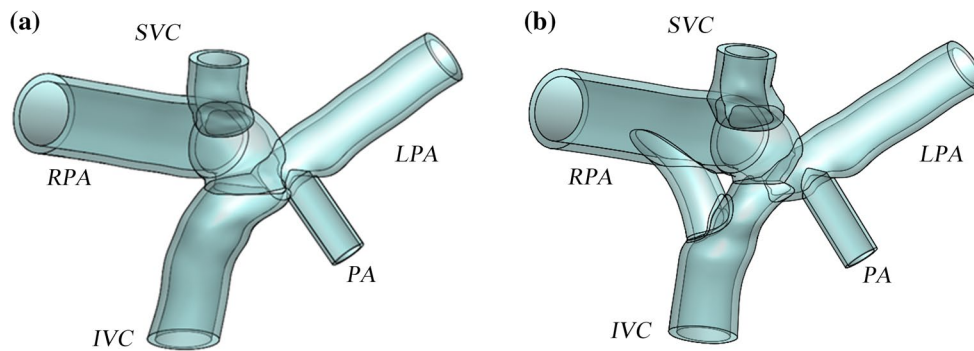


**Fig. 2** Structure model, as vessel's wall, with specific description of different vessels, **a** T-shaped geometry, **b** Y-shaped geometry

reconstruction is illustrated. In addition, inlets and outlets are virtually extended to provide the fully developed condition for inlet blood flow. In this study, the extra pulsatile flow is added to the TCPC by virtually connecting the stenosed main pulmonary artery (PA) to the main TCPC geometry. The diameter and angle of the PA are defined, through the usage of anatomical data along with the information presented by [6]. After construction of the MRI-based T-shaped geometry, the computer-generated Y-shaped geometry is constructed with anatomical and physiological considerations, Fig. 1. As mentioned before, the T-shaped geometry is obtained from a real

TCPC, while Y-shaped construction is done by constricting main IVC (as Left Arm of Y-graft) and also adding a deviational direction to the RPA (as Right Arm of Y-graft).

In order to consider the effect of vessels compliance, FSI-simulation is conducted using ADINA-FSI software. The solid geometry of T-shaped and Y-shaped models can be seen in Fig. 2. Mesh independency of the study has been investigated by increasing the number of elements and comparing the outlet velocity flux of LPA. Approximately 300,000 tetrahedral elements for fluid model and 200,000 shell elements for solid model are used, with consideration

of computational cost and precision of the simulation. The blood is considered as Newtonian fluid with a density of  $1060 \text{ kg/m}^3$  and viscosity of  $0.0035 \text{ Pa}\cdot\text{s}$ . The governing equation of FSI boundary condition is explained in the following section.

Veins and arteries have different mechanical properties. Experimental investigation of Hunter et al. [9] shows that  $3.2 \text{ mm}$  and  $200 \text{ kPa}$  are good assumptions for thickness and stiffness of pulmonary arteries, respectively. Similarly, Silver et al. [19] showed that material properties for vena cava can be considered as  $1.2 \text{ mm}$  for thickness and  $978 \text{ kPa}$  for stiffness. It is easy to deduce that arteries are more elastic compared to the veins; however, arteries are thicker than veins. Due to these characteristics, our primitive simulations showed that both vena cava and pulmonary arteries approximately have equal deformation. In other word, less stiffness of arteries than vena cava will be amended by its thicker wall. This outcome led us to consider mean mechanical properties for both vena cava and pulmonary arteries, and subsequently, it reduces the complexity of the numerical modeling. The mean thickness and stiffness of solid part are chosen to be  $2.2 \text{ mm}$  and  $590 \text{ kPa}$ , respectively.

## 2.2 Flow simulation and boundary conditions

### 2.2.1 The inlet and outlet boundary conditions

The inflow boundary condition for IVC and SVC is derived from echocardiography data of the patient. Figure 3 shows the inlet flux for both IVC and SVC during inspiration period of the cardiac cycle. As mentioned before, the fully developed flow condition is set up for both IVC and SVC by extending the entrance length.

The pulsatile flow (PF) from the heart is added to the TCPC flow through stenosed pulmonary artery. In this study, five distinct fluxes varying from 2 to 10 % of systemic flow rate are considered as PA boundary conditions. The inlet flux of PA in all five models is depicted in Fig. 4.

In the present work, constant pressure outlet is considered for both LPA and RPA. According to clinical investigations, the flow distribution of IVC and SVC between LPA and RPA has crucial impact on patient's health and has been always an important issue in Fontan surgeries [2]. Since the current study is focused on oscillation of TCPC flow, the outlet pressures are considered such that the blood flow distributes in pulmonary arteries as reported by Whitehead et al. [22]. They expressed that the average LPA flow portion is about 45 % of total of pulmonary blood flow, and this is due to the smaller size of the left lung in comparison with the right one. Our primitive results showed that this flow distribution would be established by setting RPA/LPA pressures at  $2300/2000 \text{ kPa}$  in T-shaped geometry and  $2500/2200 \text{ kPa}$  in Y-shaped geometry.

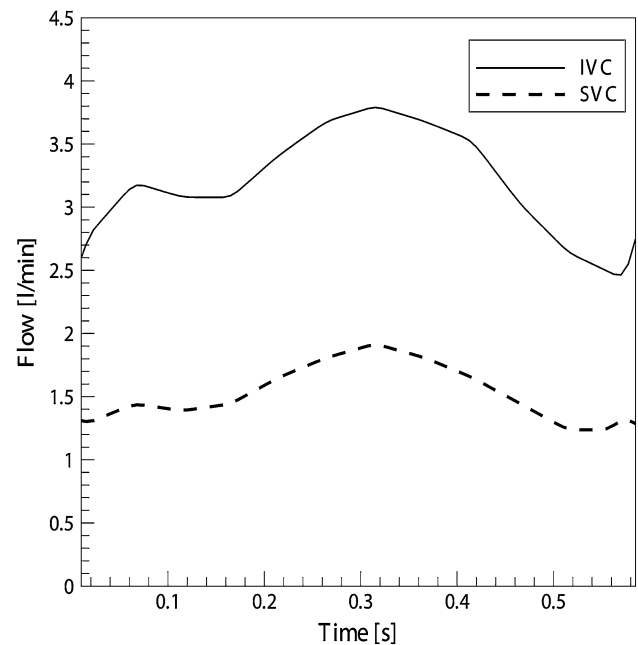


Fig. 3 The inlet flux for IVC and SVC for a cardiac cycle

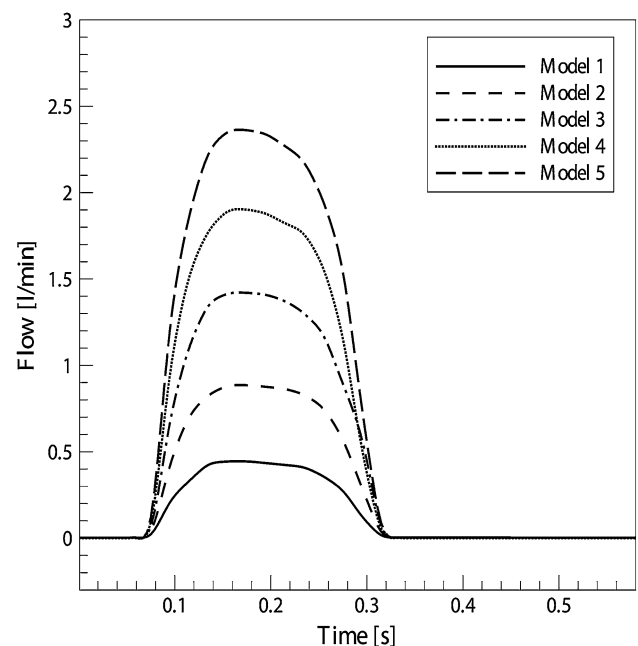


Fig. 4 The inlet flux of PA for a cardiac cycle for models 1–5

### 2.2.2 FSI boundary condition

The FSI boundary is considered for fluid–solid interfaces, where it defines the fluid load on the structure as well as the effects of the structural displacements on the fluid velocity field. Equations (1) and (2) represent the Navier–Stokes and Continuity equations for fluid region, respectively.

$$\rho_f \left( \frac{\partial \vec{u}_f}{\partial t} + \vec{u}_f \cdot \nabla \vec{u}_f \right) + \nabla p = \mu \nabla^2 \vec{u}_f \tag{1}$$

$$\nabla \cdot \vec{u}_f = 0 \tag{2}$$

In these equations,  $\rho_f$  is the density of the fluid,  $\vec{u}_f$  is the fluid velocity,  $p$  is the pressure, and  $\mu$  defines the fluid viscosity. Furthermore, the governing equation of solid region is defined by Eq. (3),

$$\rho_s \frac{\partial^2 \vec{X}_s}{\partial t^2} = \nabla \cdot \sigma_s \tag{3}$$

where  $\rho_s$  is the density of solid,  $\vec{X}_s$  is the displacement of solid elements, and  $\sigma_s$  is denotation of Cauchy stress.

Fluid and solid domains at the interface are linked to each other by FSI boundary conditions, which are represented by Eqs. (4) and (5), and kinematic and dynamic boundary conditions.

$$\frac{\partial \vec{X}_s}{\partial t} = \vec{u}_f(t) \tag{4}$$

$$\vec{n}_f \cdot \sigma_f = \vec{n}_s \cdot \sigma_s \tag{5}$$

where  $\vec{n}_f$  and  $\vec{n}_s$  are the normal vectors of fluid and solid surface at the interface boundary.

### 2.3 Determination of performance parameter

The main purpose of this study is to investigate the effect of adding pulsatile flow on pulsatility of blood flow in pulmonary arteries. In this purpose, pulsatility index (PI) is defined as a parameter for measuring the intensity of flow pulsation.

$$PI = \frac{Q_{MAX} - Q_{MIN}}{Q_{MEAN}} \tag{6}$$

In this equation,  $Q_{MAX}$  and  $Q_{MIN}$  are maximum and minimum fluxes of passing flow through pulmonary arteries. Furthermore,  $Q_{MEAN}$  is the average of blood flow throughout the cardiac cycle.

As mentioned before, TCPC leads both IVC and SVC flows to the pulmonary arteries without passing through the ventricle. Therefore, the blood pressure reduces in pulmonary arteries, which is not suitable for patient’s respiratory system. For this reason, we also computed the energy loss which is another parameter for comparison between different geometries. Total energy in each surface can be calculated by Eq. (7).

$$\dot{E}_i = \int_i \rho_f \left( \frac{p}{\rho_f} + \frac{1}{2} \vec{u}_f^2 \right) \vec{u}_f \cdot dA \tag{7}$$

This equation expresses the total energy of fluid in each cross section along the blood flow. The first term in parenthesis shows the potential energy per unit mass of fluid ( $\frac{p}{\rho_f}$ ) and the second term is the kinetic energy per unit mass ( $\frac{1}{2} \vec{u}_f^2$ ). Since the blood velocity and pressure change across the computational domain, the integration calculates the total energy of fluid in each cross section. Consequently, the rate of total energy loss in the flow field is derived as follows,

$$\begin{aligned} \dot{E}_{loss} = & \int_{IVC} \rho_f \left( \frac{p}{\rho_f} + \frac{1}{2} \vec{u}_f^2 \right) \vec{u}_f \cdot dA \\ & + \int_{SVC} \rho_f \left( \frac{p}{\rho_f} + \frac{1}{2} \vec{u}_f^2 \right) \vec{u}_f \cdot dA + \int_{PA} \rho_f \left( \frac{p}{\rho_f} + \frac{1}{2} \vec{u}_f^2 \right) \vec{u}_f \cdot dA \\ & - \int_{LPA} \rho_f \left( \frac{p}{\rho_f} + \frac{1}{2} \vec{u}_f^2 \right) \vec{u}_f \cdot dA - \int_{RPA} \rho_f \left( \frac{p}{\rho_f} + \frac{1}{2} \vec{u}_f^2 \right) \vec{u}_f \cdot dA \end{aligned} \tag{8}$$

## 3 Results

### 3.1 Pulsatility index (PI) and flow patterns

In this study, blood flow is simulated in two different types of TCPC geometry (MRI-based T-shaped and computer-generated Y-shaped), in which PA is added virtually. Each geometry experiences 5 distinct models in which the average PF increases gradually from 2 to 10 % of systemic flow by the amount of 2 % in each step (Fig. 4). The term ‘without PA’ means the original model where no extra pulsatile flow exists.

Figures 5 and 6 demonstrate the outflow flux of LPA and RPA, respectively. For better comparison between T-shaped and Y-shaped geometry, their results are superimposed. The velocity vectors for both geometries are depicted in Fig. 7. Since pulsatile blood flow increases in different models, three models are depicted in this figure. Models 3 and 5, which contain 6 and 10 % of systemic flow, are compared with the without PA model. The velocity vectors are depicted at a specific time (0.15 s) when the pulsatile blood flow reaches to the maximum intensity.

Figure 8 demonstrates the impact of increasing PF on PI value. The results show that by increasing the pulsatile flow, PI value changes in both geometries.

We have plotted wall displacement results in Fig. 9. The maximum displacement occurs in the IVC. This is because of jetting flow from PA which prevents the IVC flow. This results in increasing fluid pressure in IVC and consequently increasing wall displacement. As shown by increasing PF from a to c, the maximum wall displacement has been increased. This could be simply explained by increasing the IVC pressure by increasing the PF.

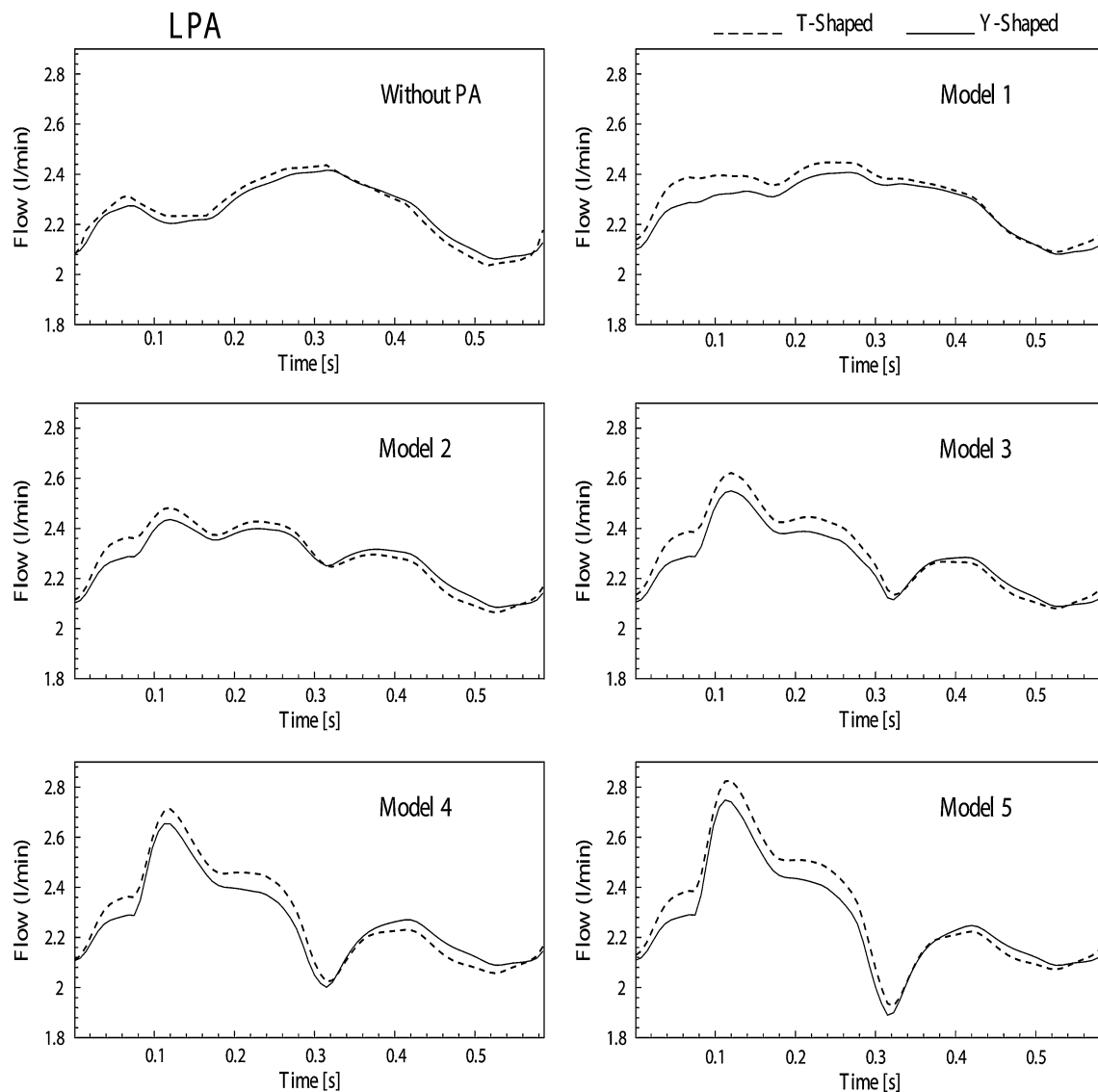


**Fig. 5** Blood flow rate in LPA for both T-shaped and Y-shaped

### 3.1.1 Left pulmonary artery

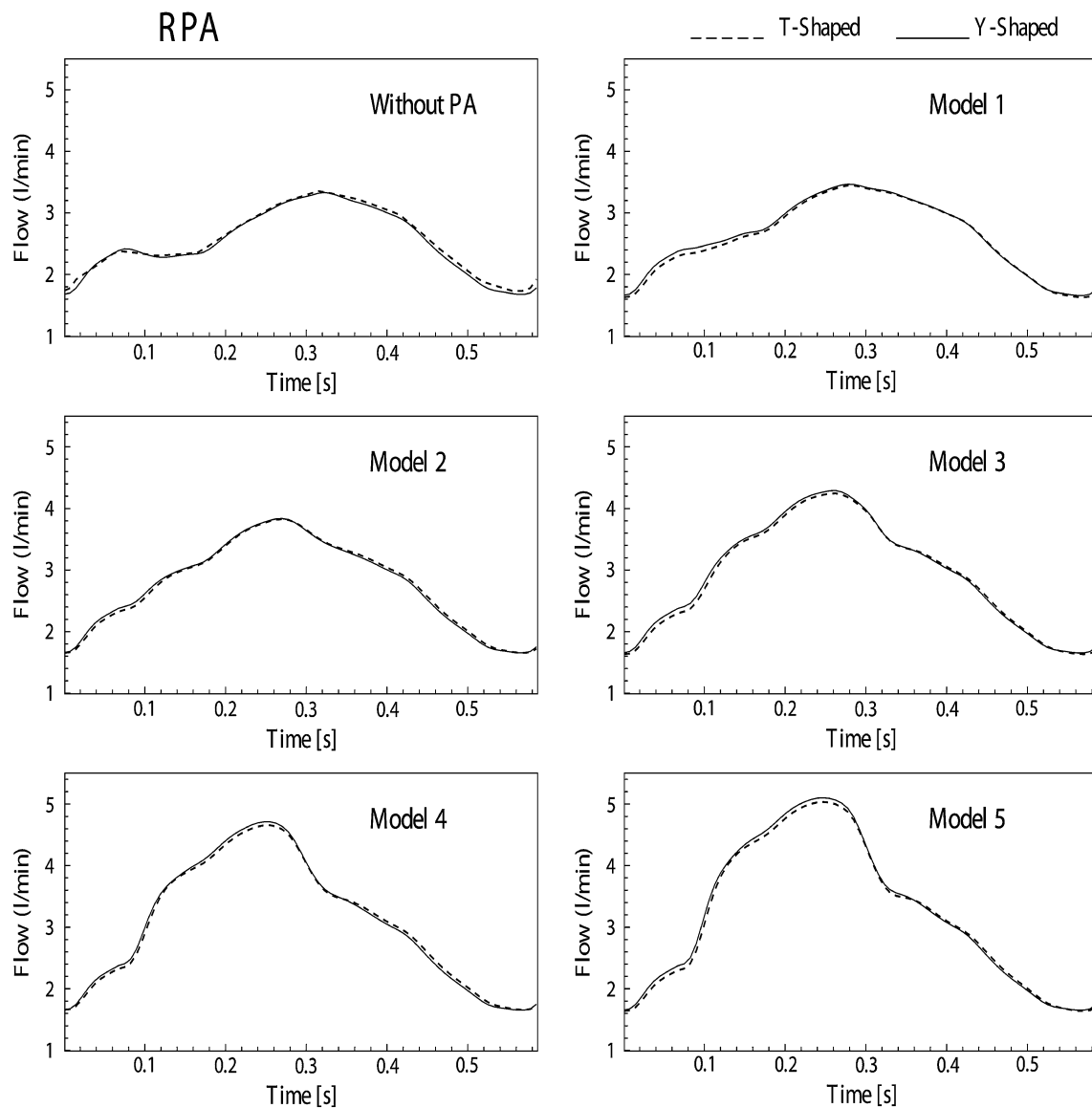
According to Fig. 5, as expected, T-shaped geometry has more LPA flow compared to Y-shaped one in all cases. This phenomenon happens due to the utilization of a Y-shaped graft for leading IVC flow toward RPA in Y-shaped geometry. Similarly, comparison between the main model (without PA) and the other 5 models (with PA) demonstrates that the LPA flow is affected by PF, in both geometries. In other word, collision of PF and LPA flow at the entrance of LPA causes deviation of IVC flow toward the RPA. This phenomenon can be seen in Fig. 7.

Figure 8 states that low inflow of PA in case 1 not only has a small effect on pulsatility of LPA flow, but also is a reason of decreasing the PI value. However, the presence of

PA in models 2–5 causes significant changes in PI value as it increases about 100 % in model 5. Comparison between two geometries in Fig. 8 shows that generally adding PF is more effective on T-shaped geometry compare to Y-shaped one. The effectiveness of T-shaped geometry is more pronounced in models 2 and 3 as the rise in PI value for the T-shaped is approximately 15 % more than the Y-shaped geometry.

### 3.1.2 Right pulmonary artery

According to Fig. 6, it can be seen that pulsatility of RPA flow in both geometries is naturally far more than LPA. This statement is also confirmed by comparing PI values presented in Fig. 8. Comparison of flow rates in RPA



**Fig. 6** Blood flow rate in RPA for both T-shaped and Y-shaped

between the two types of geometries shows that approximately both have identical PI value. As it can be seen from Fig. 8, the PI value in the RPA increases proportional to the extra flow added by PA. In contrast to LPA where the PI value changes in higher PA inflow rates, the PI value in RPA principally increases by 7 % just by adding 2 % of cardiac output to the TCPC. In addition, Fig. 8 expresses that in cases 2–5 the pulsatility index increases linearly to 64 % in comparison to the without PA model.

### 3.2 Energy loss in TCPC

Figure 10 is depicted in order to compare energy loss between the two geometries. For better perception, the calculated parameter in this figure is the percentage of energy

loss which is imposed by adding PF. We called it percentage of energy loss and defined it by following formula,

$$\begin{aligned} &\text{Percentage of Energy Loss in model } i \\ &= \frac{\dot{E}_{\text{model } i} - \dot{E}_{\text{without PA}}}{\dot{E}_{\text{without PA}}} \times 100 \% \end{aligned} \tag{9}$$

where  $\dot{E}_{\text{model } i}$  is the energy loss in the model  $i$  and  $\dot{E}_{\text{without PA}}$  is the energy loss in the without PA model.

Collision of IVC and SVC flows, especially in T-shaped geometry, is the most important factor in energy loss. Entrance of pulsatile flow from cardiac and collision of this flow with LPA blood flow reinforces the energy loss. Likewise, higher pulsatile flow from cardiac increases the energy loss in TCPC. Comparison between geometries

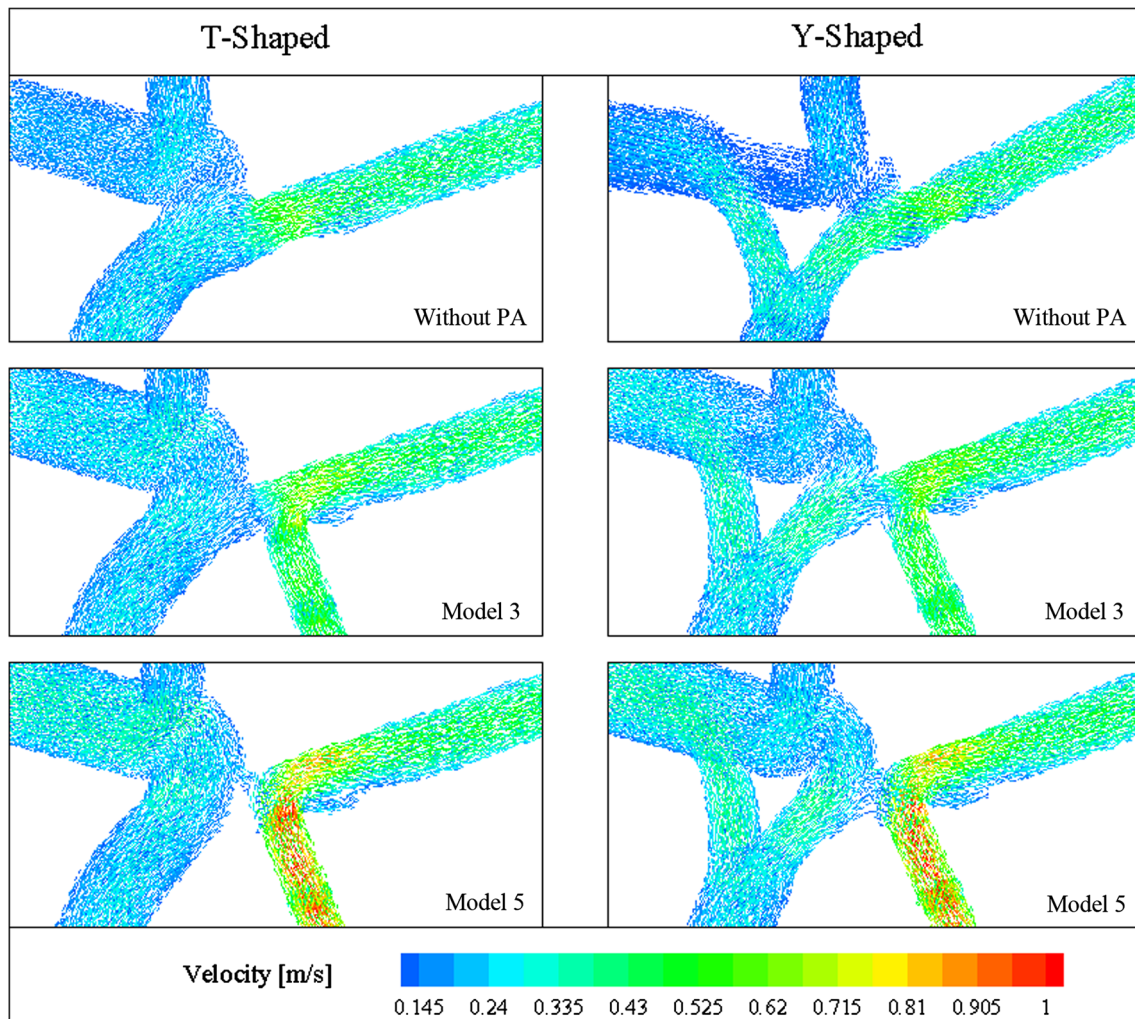


**Fig. 7** Velocity vector Plot for T-shaped and Y-shaped geometry at  $T = 0.15$  s. Increasing the intensity of pulsatile blood flow and its impact on deviation of LPA blood flow (For better observation, vectors with magnitudes lower than 0.14 m/s are removed)

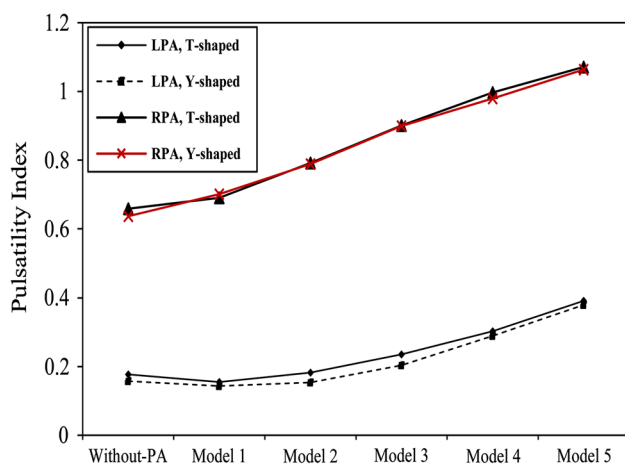


**Fig. 8** The PI Value of different models for both T-shaped and Y-shaped geometries

shows that utilization of Y-shaped geometry and consequently better combination of IVC and SVC flow reduces the energy loss significantly. For example, energy loss of Model 5 compared to without PA model in T-shaped geometry is 54 %, while it is about 27 % in Y-shaped geometry.

#### 4 Discussion

In this study, the impact of new approach to increase the pulsatility of blood flow in pulmonary arteries of a patient-specific TCPC is investigated. This approach expresses that an extra flow from the single ventricle can be added to the TCPC in order to increase the pulsatile index of the TCPC flow. According to this approach, this extra fluid will be directed to the TCPC through the stenosed main pulmonary



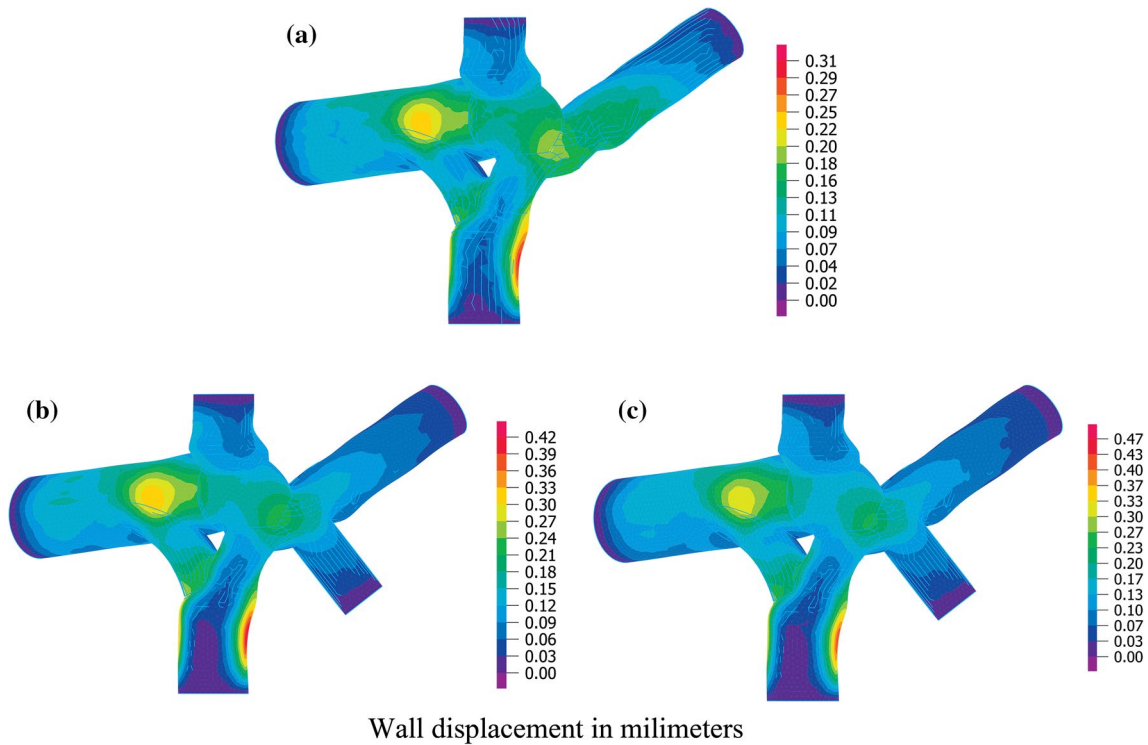


**Fig. 9** Displacement magnitude contours at  $t = 0.15$  s; **a** Y-shaped model without PF, **b** Y-shaped model 3, **c** Y-shaped model 5

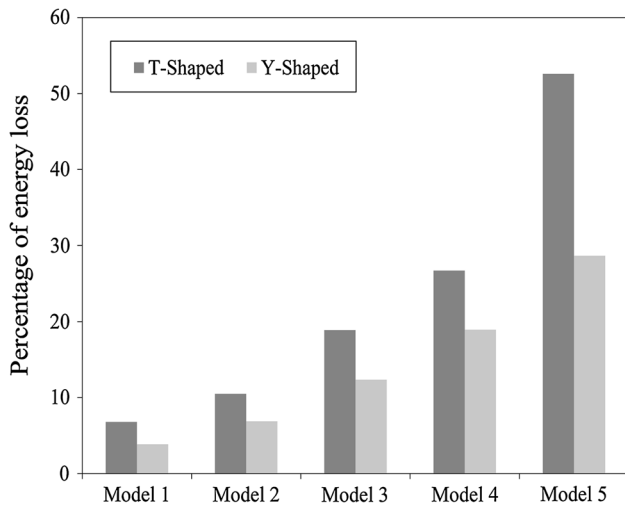


**Fig. 10** Percentage of energy loss by increasing extra pulsatile flow

artery. In this study, T-shaped and Y-shaped geometries are also compared together. The results show that adding an extra pulsatile blood flow from cardiac increases the PI value significantly in both geometry, but comparison between the two geometries shows no significant difference in PI value. On the other hand, addition of extra pulsatile flow imposes extra energy loss to the system, which makes

serious postoperative complications for the patient. The results show that using Y-shaped geometry decreases this energy loss, significantly.

Besides, the comparison between the models without PA, for both T-shaped and Y-shaped geometries, with the results reported by Marsden et al. [13], shows that the general flow pattern of blood flow and average velocity magnitude in fluid domain in our study is in agreement with Marsden results.

#### 4.1 Left pulmonary artery

Starting systolic phase of cardiac cycle and consequently addition of PF causes deviation of IVC toward RPA. This is due to collision of PF with LPA flow at the entrance of LPA. As seen in Fig. 7, this collision generates vortices which act as an obstacle for IVC flow to enter to the LPA. The velocity vectors of TCPC show how much effective is the PF on the skewness of streamlines. The more the PF is, the more the skewness of streamlines is resulted. By addition of PF, a portion of IVC flow deviates from entering to the LPA; however, this portion is partially substituted by the PF from cardiac.

Diastolic phase of cardiac cycle results in cutting off the PF; however, the IVC flow cannot enter to the LPA simultaneously. This is due to the laxation time, which is required

for settling down the formed vortices and inertia of the skewed flow. According to Fig. 5, this relaxation time is about 0.1 s.

#### 4.2 Right pulmonary artery

As mentioned before, adding PF to the TCPC causes more deviation of IVC flow to the RPA in both geometries. Furthermore, utilization of Y-graft also increases the RPA flow rate. According to the incompressibility of fluid and mass conservation law, the reduced flow of LPA should be added to the RPA; however, Fig. 6 demonstrates that the velocity profile of RPA does not change significantly. In other words, in comparison with LPA, extra flow added to the RPA is not remarked in RPA velocity profile. This is because of larger area of RPA surface in comparison with LPA. Due to this reason, utilization of Y-shaped graft does not have any significant effect on RPA velocity profile.

#### 4.3 Imposed energy loss

Single-ventricle patients have chance of survival by undergoing sequences of surgeries. These surgeries are finalized by Fontan operation in which combination of poor-oxygenated and rich-oxygenated blood is prevented by direct connection of the IVC and SVC to the pulmonary arteries. Consequently, poor-oxygenated and low pulsatile blood is directed to the pulmonary arteries without being pumped by the heart. Hence, the pressure drop and energy loss in TCPC are a crucial issue that have high influence on the health of respiratory system of the patients. In this study, the impact of directing a pulsatile flow through PA in both T-shaped and Y-shaped geometries is investigated. The results show that, although adding PF significantly increases the PI value, this approach increases energy loss which cannot be ignored. On the other hand, the results show that utilization of Y-shaped geometry reduces the energy loss by preventing of collision of IVC and SVC flows.

#### 4.4 Limitations

However; the focus of this study is on hemodynamic investigation of blood flow, the effect of PF flow on vessel wall cannot be ignored. For example, the jet flow of PF to the LPA wall, as can be seen in Fig. 7, can damage endothelial cells of the LPA and trigger formation of aneurysms on the vessel's wall. Besides, measurement of blood flow in pulmonary arteries using Doppler echocardiography or PC-MRI can be used as trustworthy validation tool which will increase the reliability of the simulation. Unfortunately, such information was not available in our study.

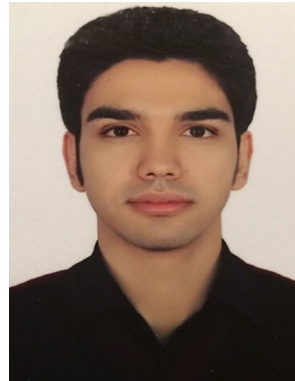
## 5 Conclusion

In this study, the hemodynamic of blood flow in a patient-specific TCPC has been investigated using a new proposed approach for increasing the pulsatility of blood flow in pulmonary arteries. In this approach, a pulsatile flow is taken from the cardiac of the patient and added to the TCPC through stenosed PA. This new approach has been tested numerically on two different types of TCPC, T-shaped and Y-shaped. To provide more realistic results, the compliance of vessels has been considered using FSI approach. The results demonstrated that PI value increases significantly by adding pulsatile flow to TCPC in both geometries, but approximately identical in both T-shaped and Y-shaped geometries. Moreover, it has been found that although this approach increases the pulsatility of blood flow in TCPC, it also imposes significant energy loss. The most important outcome of the present study is significant reduction of energy loss using Y-shaped geometry. Consequently, according to this study, Y-shaped geometry can be a beneficial replacement for T-shaped one and would have significant improvement on patient's health as well. We believe more comprehensive study is necessary to make a solid conclusion about this new procedure; however, this study provides a new inside for solving an old problem.

## References

1. Berdat PA, Belli E, Lacour-Gayet F, Planché C, Serraf A (2005) Additional pulmonary blood flow has no adverse effect on outcome after bidirectional cavopulmonary anastomosis. *Ann Thorac Surg* 79:29–36
2. de Zelicourt DA, Marsden A, Fogel MA, Yoganatham AP (2010) Imaging and patient-specific simulations for the Fontan surgery: Current methodologies and clinical applications. *Progress Pediatric Cardiol* 30:31–44
3. DeGroff C, Birnbaum B, Shandas R, Orlando W, Hertzberg J (2005) Computational simulations of the total cavo-pulmonary connection: insights in optimizing numerical solutions. *Med Eng Phys* 27:135–146
4. Fogel MA, Weinberg PM, Rychik J, Hubbard A, Jacobs M, Spray TL et al (1999) Caval contribution to flow in the branch pulmonary arteries of fontan patients with a novel application of magnetic resonance presaturation pulse. *Circulation* 99:1215–1221
5. Gersony WM (2008) Fontan operation after 3 decades what we have learned. *Circulation* 117:13–15
6. Ghoreyshi M, Saeidi MS, Nabavi MA, Firoozabadi B, Shabani R (2012) Numerical investigation of antegrade flow effects on flow pulsations in Fontan operation. *Int J Biomed Eng Technol* 10
7. Gray RG, Altmann K, Mosca RS, Prakash A, Williams IA, Quaegebeur JM et al (2007) Persistent antegrade pulmonary blood flow post-glenn does not alter early post-Fontan outcomes in single-ventricle patients. *Ann Thorac Surg* 84:888–893
8. Hjortdal VE, Emmesten K, Stenbog E (2003) Effects of exercise and respiration on blood flow in total cavopulmonary

- connection: a real-time magnetic resonance flow study. *Circulation* 108:1227–1231
9. Hunter KS, Albiets JA, Lee PF, Lanning CJ, Lammers SR, Hofmeister SH et al (2010) In vivo measurement of proximal pulmonary artery elastic modulus in the neonatal calf model of pulmonary hypertension: development and ex vivo validation. *J Appl Physiol* 108:968–975
  10. Krishnankuttyrema R, Dasi LP, Pekkan K, Sundareswaran K, Fogel M, Sharma S et al (2008) Quantitative analysis of extracardiac versus intraatrial fontan anatomic geometries. *Ann Thorac Surg* 85:810–817
  11. Liu Y, Pekkan K, Jones SC, Yoganathan AP (2004) The effects of different mesh generation methods on computational fluid dynamic analysis and power loss assessment in total cavopulmonary connection. *J Biomech Eng* 126:594–603
  12. Marsden AL, Vignon-Clementel IE, Chan FP, Feinstein JA, Taylor CA (2007) Effects of exercise and respiration on hemodynamic efficiency in CFD simulations of the total cavopulmonary connection. *Ann Biomed Eng* 35:250–263
  13. Marsden AL, Bernstein AJ, Reddy VM, Shadden SC, Spilker RL, Chan FP et al (2009) Evaluation of a novel Y-shaped extracardiac Fontan baffle using computational fluid dynamics. *J Thorac Cardiovasc Surgery* 137:394–403.e2
  14. Oghaz HR, Firoozabadi B, Saidi MS, Monjezi M, Navabi Shirazi MA, Malakan Rad E (2015) Evaluation of a novel extra-cardiac Fontan procedure with implantation of a biocompatible membrane. *IRBM* 36(5):287–292
  15. Orlando W, Shandas R, DeGroff C (2006) Efficiency differences in computational simulations of the total cavo-pulmonary circulation with and without compliant vessel walls. *Comput Methods Programs Biomed* 81:220–227
  16. Parker SE, Mai CT, Canfield MA, Rickard R, Wang Y, Meyer RE et al (2010) Updated national birth prevalence estimates for selected birth defects in the United States, 2004–2006. *Birth Defects Res A* 88:1008–1016
  17. Pekkan K, Whited B, Kanter K, Sharma S, De Zelicourt DA, Sundareswaran K et al (2008) Patient-specific surgical planning and hemodynamic computational fluid dynamics optimization through free-form haptic anatomy editing tool (SURGEM). *Med Biol Eng Comput* 11:1139–1152
  18. Rajabzadeh HR, Firoozabadi B, Saidi MS, Sohrabi S, Mehr SMN (2013) Numerical modeling of pulsating inflow to the pulmonary arteries in TCPC morphology using FSI approach. In: *ASME 2013 International mechanical engineering congress and exposition*, pp V03AT03A058–V03AT03A058
  19. Silver FH, Snowhill PB, Foran DJ (2003) Mechanical behavior of vessel wall: a comparative study of aorta, vena cava, and carotid artery. *Ann Biomed Eng* 31:793–803
  20. Throckmorton AL, Ballman KK, Myers CD, Frankel SH, Brown JW, Rodefeld MD (2008) Performance of a 3-bladed propeller pump to provide cavopulmonary assist in the failing Fontan circulation. *Ann Thorac Surg* 86:1343–1347
  21. van de Wal HJCM, Ouknine R, Tamisier D, Levy M, Vouhe PR, Leca F (1999) Bi-directional cavopulmonary shunt: is accessory pulsatile flow, good or bad? *Eur J Cardiothorac Surg* 16:104–110
  22. Whitehead KK, Sundareswaran KS, Park WJ, Harris MA, Yoganathan AP, Fogel MA (2009) Blood flow distribution in a large series of patients having the fontan operation: a cardiac magnetic resonance velocity mapping study. *J Thorac Cardiovasc Surgery* 138:96–102
  23. Yang WG, Feinstein JA, Marsden AL (2010) Constrained optimization of an idealized Y-shaped baffle for the Fontan surgery at rest and exercise. *Comput Meth App Mech Eng* 199:2135–2149
  24. Yoshida M, Yamaguchi M, Yoshimura N, Murakami H, Matsuhisa H, Okita Y (2005) Appropriate additional pulmonary blood flow at the bidirectional Glenn procedure is useful for completion of total cavopulmonary connection. *Ann Thorac Surg* 80:976–981



**Hamidreza Rajabzadeh-Oghaz** received his M.S. degree from Sharif University, Tehran, in 2014. Currently, he is Ph.D. Student at University at Buffalo. He is Research Assistant at Toshiba Stroke and Vascular Research Center, Buffalo, USA. His primary research concentrates on numerical simulation of cardiovascular disease such as single ventricle and cerebral aneurysms.



**Bahar Firoozabadi** received her Ph.D. in Mechanical Engineering from Sharif University of Technology, Tehran, where she is now Professor at the School of Mechanical Engineering. Her research interests include: Fluid Mechanics in density currents, presently focusing on biofluid mechanics and cell biology simulation as well. She teaches Fluid Mechanics and Gas Dynamics to undergraduates and Viscous Flow, Advanced Fluid Mechanics, Continuum Mechanics and Bio-

fluid Mechanics to graduate students.



**Mohammad Said Saidi** received his Ph.D. in Nuclear Engineering from Massachusetts Institute of Technology, USA. He is now Professor at the School of Mechanical Engineering at Sharif University of Technology, Tehran. His research concentrates on Computational Fluid Dynamics and Simulation of micro- and macro-multiphase flows in human body.



**Mojdeh Monjezi** is Ph.D. Student at Sharif University, Tehran, Iran. Her research interest concentrates in bio-fluid mechanics.



**Elaheh Malakan Rad** is Associate Professor of Pediatric interventional cardiology at Pediatric Center of Excellence. Currently, she is a deputy of educational affairs of department of pediatrics of Tehran University of Medical Sciences.



**Mohammad Ali Navabi Shirazi** is Professor of Cardiac Surgery at Tehran University of Medical Sciences. Since 1990, he performed more than 4800 surgical procedures including 4100 procedures for congenital heart defects.